Breaking and Re-Forming the Disulfide Bond at the High-Potential, Respiratory-Type Rieske [2Fe-2S] Center of *Thermus thermophilus*: Characterization of the Sulfhydryl State by Protein-Film Voltammetry†

Yanbing Zu,‡ James A. Fee,§ and Judy Hirst*,‡

Medical Research Council Dunn Human Nutrition Unit, Wellcome Trust/MRC Building, Hills Road, Cambridge CB2 2XY, U.K., Division of Biology, University of California at San Diego, La Jolla, California 92093, and Department of Molecular Biology, The Scripps Research Institute, 10550 North Torrey Pines Road, La Jolla, California 92037

Received August 6, 2002; Revised Manuscript Received September 20, 2002

ABSTRACT: A disulfide bond, adjacent to the [2Fe-2S] cluster, is conserved in all high-potential Rieske proteins from the respiratory and photosynthetic cytochrome bc_1 and b_6f complexes but is absent from the low-potential, bacterial dioxygenase Rieske proteins. The role of the disulfide is unclear, since cysteine mutants have resulted in only apoprotein. The high stability of the soluble *Thermus thermophilus* Rieske protein permits chemical reduction of the disulfide bond and characterization of the sulfhydryl (dithiol) form by protein-film voltammetry. The effect of disulfide reduction on the cluster potential is small ($\Delta E^{0\prime} \leq -0.04$ V) and attributed to relaxation of the disulfide tether between the protein loops ligating the cluster, including possible mechanical strain release and hydrogen-bonding modification. Above pH 6 an additional decrease in potential of the sulfhydryl form is assigned to the nearby negatively charged thiolates ($\Delta E^{0\prime}$ −0.16 to −0.12 V); the histidine-ligand nitrogen p*K*s are correspondingly increased. Entropies of reduction for the native and dithiolate forms are equal (-48 ± 5 J K^{-1} mol^{-1}, pH 7−8); thus changes in reduction potential are enthalpic in origin. Following sulfhydryl alkylation the cluster redox properties mirror those of the native protein ($\Delta E^{0\prime} \sim -0.1$ V) over all pHs. While a sustained electrode potential of −0.85 V fails to reduce the disulfide, the free sulfhydryls recombine upon an oxidative excursion, at low pH, to restore the native redox properties. This unique behavior is attributed to preorganization of the two thiolate groups upon uptake of one or more protons by the sulfhydryl pair.

Rieske iron−sulfur proteins contain a 2Fe-2S center with unique ligand coordination, one of the two iron centers being coordinated by two cysteine residues and the other by two histidine residues (*1*−*4*). They are essential components of the respiratory cytochrome bc_1 and photosynthetic cytochrome b_6f complexes and of the bacterial dioxygenase systems which initiate the degradation of aromatic compounds. Rieske centers adopt a wide range of reduction potential, encompassing a total spread of around 500 mV at pH 7 (*1*, *5*, *6*), and how their reduction potentials are determined is therefore a question of much contemporary interest. Rieske clusters within cytochrome bc_1 and b_6f complexes display very positive reduction potentials, typically around +300 mV at pH 7 for a complex that oxidizes ubiquinol, and a strong pH dependence. Menaquinone-utilizing organisms such as *Thermus thermophilus* have lower potentials of around +150 mV at pH 7, in line with the difference between their quinone potentials, and retain the pH dependence (*1*, *7*). This 150 mV decrease appears to be due to the absence of one cluster-serine hydrogen bond; the serine residue is conserved in ubiquinone-utilizing organisms but is replaced by glycine or alanine when menaquinone is used (*8*, *9*). The pH dependence, of ∼450 mV over ∼5 pH units for the *T. thermophilus* Rieske protein (*7*), is ascribed to the deprotonation of the two histidine cluster ligands (*1*, *10*, *11*). In contrast, Rieske clusters in bacterial dioxygenase systems have much lower reduction potentials, around −150 mV, which are pH-independent over the physiological range (*1*, *5*, *12*).

Atomic resolution structural models are available for both major classes of Rieske protein, enabling evaluation of the factors which may contribute to producing these alternative characteristics. The structures of the soluble fragments of the high-potential Rieske proteins from the cytochrome bc_1 complex of bovine heart mitochondria (*2*), the cytochrome b_6f complex of spinach chloroplasts (*13*), and the terminal oxidase SoxM supercomplex of *Sulfolobus acidocaldarius* (*14*) show that each protein has two subdomains, a cluster-binding subdomain and a larger basal subdomain. The cluster-binding subdomains (residues 137−180 for the bovine protein) are virtually identical (though SoxF has a 12-residue insertion), whereas the basal subdomains have a common overall topology but are much more variant (*13*, *14*). Figure 1 depicts the typical cluster environment of the mitochondrial protein (*2*).[1] The cluster-binding subdomain is composed of three loops between β-sheets; loops β4−β5 and β6−β7 each

† This work was supported by The Medical Research Council and by NIH Grant GM35342.

* To whom correspondence should be addressed. Tel: +44 1223 252810. Fax: +44 1223 252815. E-mail: jh@mrc-dunn.cam.ac.uk.

‡ Medical Research Council Dunn Human Nutrition Unit.

§ University of California at San Diego and The Scripps Research Institute.

10.1021/bi026589r CCC: $22.00
Published on Web 10/31/2002

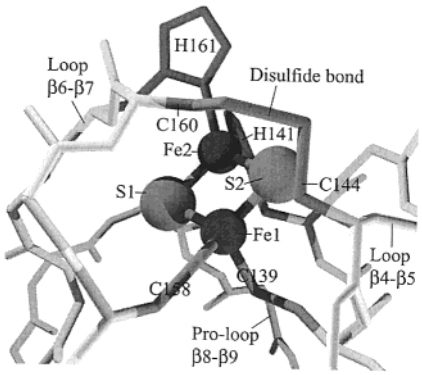

FIGURE 1: Structure of the protein around the Rieske cluster, taken from the structure of the Rieske protein from bovine heart mitochondria (PDB code 1RIE) (*2*). The cluster is ligated by two loops, $\beta4-\beta5$ and $\beta6-\beta7$, connected by the disulfide bridge between Cys 144 and Cys 160.

carry two cluster ligands and are tethered together by a disulfide bond, and the "Pro-loop" $\beta8-\beta9$ is also crucial for cluster stability. The cluster is located at the tip of the fold, close to but protected from solvent, though both titratable histidine nitrogens are solvent exposed. The low-potential Rieske ferredoxin from the biphenyl dioxygenase of *Burkholderia* sp. strain LB400 (*16*) also has a very similar cluster-binding subdomain, with the basal subdomain bearing most similarity to the mitochondrial homologue.

The high structural similarity between the cluster-binding subdomains of the high- and low-potential Rieske proteins rules out the possibility that changes in cluster solvent accessibility determine their widely different properties [previously suggested from the structure of naphthalene 1,2-dioxygenase, in which the low-potential Rieske center is buried in the protein interior (*17*)]. Instead, calculations of electrostatic potentials have suggested that the redox potential of the biphenyl dioxygenase ferredoxin cluster is decreased because it lacks five of the side chain or backbone interactions which stabilize the reduced state of the Rieske cluster in the mitochondrial and chloroplast proteins (*16*). One further clear distinction is the presence of a disulfide bridge, shown in Figure 1, located immediately adjacent to the Rieske cluster and connecting loop $\beta4-\beta5$ to loop $\beta6-\beta7$ in only the high-potential Rieske proteins (*2*). The two disulfide-bonding cysteines are fully conserved in all of these proteins within the cluster sequence binding motif:

$$\underline{\text{Cys}}\text{-X-}\underline{\text{His}}\text{-X-Gly-Cys*-X}_{12-44}\text{-}\underline{\text{Cys}}\text{-X-Cys*-}\underline{\text{His}}$$

(residues underlined are cluster ligands; disulfide-bonding residues are marked by an asterisk) (*1*). Site-directed mutants of the cytochrome bc_1 complexes of *Saccharomyces cerevisae*, *Rhodobacter capsulatus*, and *Rhodobacter sphaeroides* have shown that substitution of any one of the four conserved cysteine residues results in the absence of the cluster, indicating the disulfide bridge to play an important role in cluster stability or construction (*18*−*20*). However, this assumption is challenged by the low-potential ferredoxins, which lack the disulfide but which present a stable cluster, within a virtually identical structure. In all three high-potential Rieske structures, the disulfide bridge is close to van der Waals contact with the iron−sulfur center; for the bovine protein the closest approach is 4.0 Å between the sulfur of Cys144 and the cluster sulfide S2. It is therefore likely that the two redox groups interact, such that the redox and protonation states of one affects the redox and protonation properties of the other. Indeed, chloroplast ferredoxin:thioredoxin reductase uses the direct interaction of a [4Fe-4S] cluster to stabilize the one-electron reduced form of an active site disulfide (*21*−*23*), and a related mechanism has recently been proposed for the heterodisulfide reductase from *Methanothermobacter marburgensis* (*24*).

In a previous publication (*7*), the application of protein-film voltammetry (PFV)[2] (*25*, *26*) to quantify the thermodynamics of proton-coupled electron transfer by the soluble bc_1-type Rieske protein fragment from *Thermus thermophilus* (*4*, *27*) was described. For PFV a film of protein molecules, ideally a monolayer, is formed upon a pyrolytic graphite edge electrode, placed into the experimental solution, and the potential is scanned reversibly between two limits. Thus the reduction potentials of redox centers can be measured rapidly, under a wide range of conditions, using only very small amounts of sample. For the *T. thermophilus* Rieske protein reversible voltammetry could be recorded from pH 3 to pH 14, and two p*K* values were determined for each oxidation state of the iron−sulfur cluster. Additionally, the reduction potential of each protonation state was quantified, providing a complete thermodynamic "map" for the redox-coupled protonation of the Rieske cluster (*7*). This publication now describes how the high stability of the *T. thermophilus* Rieske protein permits the disulfide bond to be chemically reduced while retaining an intact iron−sulfur cluster, thus allowing any changes in the pH-dependent reduction potential to be quantified. Although the disulfide cannot be reduced electrochemically, oxidation of the two sulfhydryl groups, to recover the native protein, is observed with a rate strongly dependent upon both electrode potential (or cluster oxidation state) and pH. These latter experiments exploit the redox properties of the iron−sulfur center as an accurate and real-time "on-site" reporter of the status of the disulfide bond.

EXPERIMENTAL PROCEDURES

Expression and Purification of the T. thermophilus Soluble Rieske Protein Fragment. The soluble domain (residues 37−210) of the Rieske protein from *T. thermophilus* (*27*) was obtained by heterologous overexpression in *Escherichia coli*. A detailed description of the overexpression and purification protocols, along with the atomic resolution structure of the *T. thermophilus* Rieske protein fragment, is in preparation and will be published separately (*15*). Protein purity was confirmed by SDS−PAGE analysis, and the N-terminal sequence was verified by automated Edman degradation on a Model 494 Procise protein sequencer (Applied Biosystems,

[1] The structure of the *T. thermophilus* Rieske protein has recently been solved, and a manuscript is in preparation (*15*). As predicted, the cluster-binding subdomain has the same fold as described for the published high-potential Rieske protein structures, with the disulfide bridge located in exactly the position expected.

[2] Abbreviations: BAL, British Anti-Lewisite; BMPA, *N*-β-maleimidopropionic acid; DTT, dithiothreitol; EPR, electron paramagnetic resonance; ESI-MS, electrospray ionization mass spectrometry; IAA, iodoacetamide; NBM, *N*-benzylmaleimide; NEM, *N*-ethylmaleimide; PDI, protein disulfide isomerase; PFV, protein-film voltammetry; TAT, twin arginine translocation (pathway); TCEP, tris(2-carboxyethyl)-phosphine hydrochloride.

U.K.), following transfer from an SDS−PAGE gel to an Immobilon P membrane (Millipore, Bedford, MA) in a solution of 25 mM tris(hydroxymethyl)aminomethane, 192 mM glycine, and 10% methanol.

Protein-Film Voltammetry. Reduction potentials were measured using protein-film voltammetry. To prepare the film, protein solution (~200 μM, pH 7.5) was applied directly to a fresh pyrolytic graphite edge electrode surface [polished with 1 μm alumina (Buehler, Lake Bluff, IL), sonicated, and rinsed thoroughly with Millipore water] and then placed into solution in an all-glass electrochemical cell. A standard calomel reference electrode was separated from the cell by a Luggin capillary, and all potentials were corrected to the standard hydrogen electrode scale (*28*). The cell was encased in a Faraday cage to minimize electrical noise, thermostated with a water jacket, and housed in an anaerobic glovebox (O_2 ~1 ppm; Belle Technology, Portesham, U.K.). Remaining electrical noise was removed by Fourier transformation, provided that signal and noise were on sufficiently separate time scales. Analogue-scan cyclic voltammetry was performed using a PGSTAT30 Autolab electrochemical analyzer (Eco-chemie, Utrecht, The Netherlands) equipped with ADC750 and Scan-Gen modules. Background currents, attributable to electrode capacitance and surface chemistry, were subtracted using an in-house analysis program (courtesy of Dr. H. A. Heering) which fits a cubic spline function to the baseline in regions sufficiently far from the peak and assumes continuation of a similar, smooth function throughout the peak region. Solution pH values were controlled by mixtures of four buffers at 10 mM concentration (total 40 mM) chosen, depending on the pH, from sodium acetate, 4-(2-hydroxyethyl)piperazine-1-ethanesulfonic acid (HEPES), 2-morpholinoethanesulfonic acid (MES), *N*-[tris(hydroxymethyl)methyl]-3-aminopropanesulfonic acid (TAPS), 3-(cyclohexylamino)-1-propanesulfonic acid (CAPS), and sodium phosphate; volumetric solutions of NaOH were used above pH 13. The pH of each solution was checked immediately following measurement, at the experimental temperature, by using a standard glass electrode, calibrated at temperature according to known standards (*29*). NaOH (1 M) was used as a pH 14 standard. The effects of high Na^+ concentration were corrected by standard formulas (*28*). All potentials were confirmed to be independent of the buffer composition, and NaCl, generally at 2 M concentration, was used as the supporting electrolyte (*7*). Entropies of reduction were calculated from the variation of reduction potential with temperature at a specific pH value (*30*). The temperature of the reference electrode was held constant to preclude any additional contribution to ΔS^0: thus $\Delta S^0_{obs} = \Delta S^0_{FeS}$.

Reduction of the Disulfide Bond and Alkylation of Free Sulfhydryl Groups. The disulfide bond was reduced by incubation with TCEP [tris(2-carboxyethyl)phosphine hydrochloride, Perbio Science U.K. Ltd., Cheshire], and the progress of the reaction was monitored by extracting small aliquots from the reaction mixture and assessing the relative sizes of the reactant and product signals (see below). Conditions were therefore selected which produced a completely reduced sample but which minimized the reaction time and, therefore, protein denaturation. Specifically, a solution containing ~200 μM Rieske protein (pH 7.5) and 10 mM TCEP (added from a 50 mM stock, pH 7) was incubated anaerobically at 60 °C for 1 h; this produced a completely reduced sample stable for at least 24 h when kept anaerobically at 4 °C. Free thiol groups were alkylated, following reduction by TCEP, by *N*-ethylmaleimide (NEM, Sigma-Aldrich), *N*-β-maleimidopropionic acid (BMPA; Perbio Science U.K. Ltd., Cheshire), iodoacetamide (IAA; Sigma-Aldrich), or *N*-benzylmaleimide (NBM; Sigma-Aldrich). The reduced protein was incubated at room temperature with 100 mM alkylating reagent, added from a 200 mM aqueous stock solution; by monitoring the reaction with voltammetry 1 h was found sufficient to alkylate the free sulfhydryls completely. The extent of alkylation was also investigated by electrospray ionization mass spectrometry (ESI-MS; see below).

UV−Visible and EPR Spectroscopy. UV−visible spectra were recorded using a small-volume (50 μL) quartz SUPRASIL precision cuvette (Hellma, Southend-on-Sea, U.K.), sealed under anaerobic conditions, and a UV-1601 Shimadzu spectrometer. Electron paramagnetic resonance (EPR) spectra were recorded on a Bruker EMX X-band spectrometer using an ER 4119HS high-sensitivity cavity maintained at low temperature by a ESR900 continuous-flow liquid helium cryostat (Oxford Instruments, Abingdon, U.K.); the sample temperature was measured with a calibrated Cernox resistor (Lake Shore Cryotronics Inc., OH). Power levels were determined to be below microwave saturation, and 100 kHz field modulation amplitudes were chosen to avoid signal distortion and rapid-passage effects.

Protein Mass Measurement. Samples were applied to a reverse-phase HPLC Aquapore RP-300 column (Perkin-Elmer) to denature and desalt them, eluted by an acetonitrile gradient in 0.1% TFA, and examined using ESI-MS in the positive ion mode. The Sciex API III$^+$ triple quadrupole mass spectrometer was tuned and calibrated with a mixture of poly(propylene glycol)s over the range of *m*/*z* 59−2010 and checked using horse heart myoglobin (average mass 16951.4 Da). Samples were introduced, via a Rheodyne loop, into a stream (3 μL min^{-1}) of 50% aqueous acetonitrile and spectra recorded by scanning the first quadrupole (Q1) from *m*/*z* 700 to *m*/*z* 1700.

RESULTS

pH-Dependent Reduction Potential of the T. thermophilus Rieske Protein. Reversible oxidation and reduction of the soluble Rieske domain of *T. thermophilus* was observed by adsorbing the protein directly upon a freshly polished pyrolytic graphite-edge electrode surface. Upon cycling the electrode potential, clearly defined oxidation and reduction waves were observed; these signals were not observed in the absence of adsorbed protein. At slow scan rates the response was reversible, since peak half-height widths and separations were close to their Nernstian (equilibrium) values (typically 110 and 20 mV, respectively), reflecting facile exchange of electrons between adsorbed protein redox centers and the electrode (*31*). Protein coverage (determined from peak areas) was maximally 2×10^{-11} mol cm^{-2}, corresponding to formation of a monolayer or submonolayer of protein. Typical examples are shown in Figure 2A, which presents raw data along with "background-subtracted" signals, corrected for electrode capacitance. Notably, reversible voltammetry could also be observed at unusually high pH, up to pH 14 (*7*). At these alkaline pHs the signals were still clearly

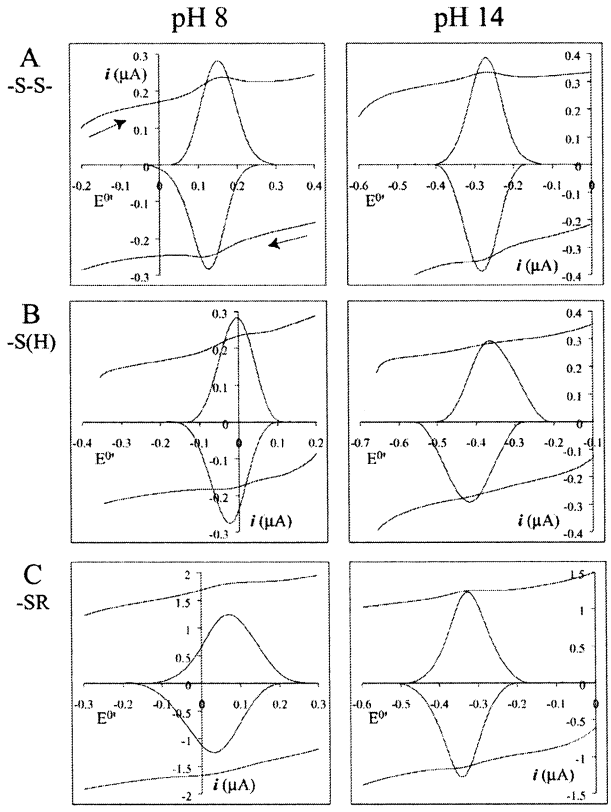

FIGURE 2: Examples of voltammograms recorded for the three main states of the Rieske protein: (A) unmodified Rieske protein, (B) with the disulfide reduced by TCEP, and (C) with the free sulfhydryl groups modified with NEM. In each case two examples are presented: at pH 8 [8.04, 8.13, and 7.98 for (A), (B), and (C), respectively] and at pH 14. The raw data are presented on the same graph as background-subtracted voltammograms which show more clearly the signals resulting from the reversible oxidation and reduction of the Rieske center. For these peaks, the intensity has been corrected so that in all cases a perfect Nernstian peak height would be equivalent to the *y*-axis span; thus peak areas from graph to graph are equivalent. The *x*-axis covers 0.6 V in each case, though the ranges are shifted to allow for the different peak potentials. All voltammograms are recorded at 20 mV s^{-1}, 20 °C; solution conditions are as described in Experimental Procedures using 2 M NaCl.

visible, and repeatedly switching the electrode, carrying the protein film, between solutions of high and low pH did not affect the recorded potentials. This demonstrated that the strongly alkaline solutions did not result in irreversible damage to the protein. The average peak potential, measured under reversible conditions, is equivalent to the reduction potential of the redox center, and Figure 3 includes the pH dependence for the reduction potential of native *T. thermophilus* Rieske protein between pH 3 and pH 14. As described previously (*7*) the pH dependence can be modeled using eq 1 (*32*) to determine the p*K* values and reduction potentials,

$$E^{0\prime}_{\text{obs}} = E^{0\prime}_{\text{alk}} - \frac{RT}{F}\ln\left[\left(1 + \frac{a_{H^+}}{K_{ox2}} + \frac{a_{H^+}^2}{K_{ox1}K_{ox2}}\right)\Big/ \left(1 + \frac{a_{H^+}}{K_{red2}} + \frac{a_{H^+}^2}{K_{red1}K_{red2}}\right)\right] \quad (1)$$

as defined in Scheme 1, which describe conversion between each state of the system (Table 2). Fits to the data are included in Figure 3. As previously discussed (*7*), several

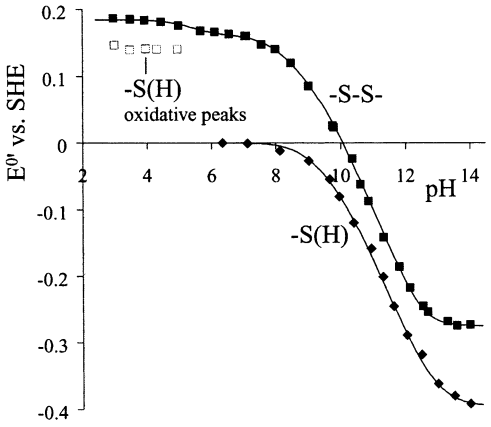

FIGURE 3: Variation of reduction potential with pH for the native Rieske protein (■) and with the disulfide bond reduced by TCEP (◆). The oxidative peak positions recorded at low pH for the TCEP-reduced protein are also shown (□). Fits to the data are using eq 1 and Scheme 1, and *E* and p*K* values are given in Table 2. The feature at pH ~5 in the curve for the native protein is due to reversal of the protein charge at the isopotential point (4.7). Experimental conditions are as for Figure 2.

Scheme 1: Thermodynamic Square Scheme Showing Oxidation and Protonation States of the Rieske Cluster and Parameters Which Describe Their Interconversion

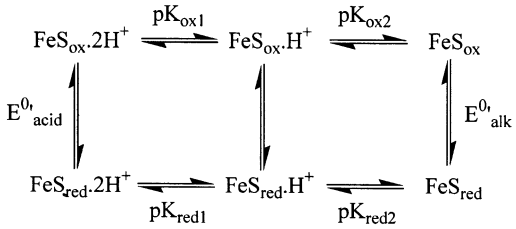

conclusions may be drawn: (i) Between pH 10 and pH 12 the gradient of the curve is −116 mV; thus two protons are transferred for every electron. Between pH 8.2 and pH 9.2 the gradient is close to −58 mV, reflecting the stability of the singly protonated state. (ii) In Scheme 1, pK_{ox1} and pK_{ox2} refer to values for the cluster in the oxidized state, and pK_{red1} and pK_{red2} refer to values in the reduced state; these p*K* values are assigned to deprotonation of the two cluster-ligating histidine residues (*1*, *10*, *11*). (iii) The reduction potential of the cluster is strongly dependent on protonation state, falling almost 450 mV from the acid to the alkaline limit. (iv) Reduction potentials are ionic strength dependent, particularly below pH 8. Previously, this behavior was ascribed to the influence of a weakly coupled protonation distant from the cluster site (*7*). However, we now believe it is due to changes in protein charge with pH, since the measured value of the isopotential point, 4.7 (*4*), agrees well with the pH (~5) at which the potential switches from increasing, to decreasing, with decreasing ionic strength. Similar behavior has been described in detail for the [2Fe-2S] cluster of the overexpressed 24 kDa subunit of NADH: (ubi)quinone oxidoreductase (complex I) (*33*). Since this complication can largely be removed by using high ionic strengths, all experiments described here were carried out in 2 M NaCl, thus displaying simply the pH-dependent properties of the Rieske cluster.

The Rieske Center Reduction Potential Responds to Disulfide Bond Reduction. All attempts to reduce the disulfide bond electrochemically failed,[3] even the application

Table 1: Reduction Potentials (V vs SHE) at Four pH Values, Representative of the Accessible pH Range, Recorded for the Rieske Center under a Variety of Conditions[a]

	pH 5	pH 8	pH 11	pH 14
native	0.175	0.140	−0.097	−0.275
heated without TCEP	0.174 (−0.001)	0.138 (−0.002)	−0.097 (0.0)	−0.273 (+0.002)
ascorbate reduced	0.173 (−0.002)	0.141 (+0.001)	−0.097 (0.0)	−0.277 (−0.002)
NEM only	0.171 (−0.004)	0.145 (+0.005)	−0.101 (−0.004)	−0.278 (−0.003)
BMPA only	0.173 (−0.002)	0.140 (0.0)	−0.095 (+0.002)	−0.274 (+0.001)
recombined	0.174 (−0.001)	0.142 (+0.002)	−0.095 (+0.002)	−0.274 (+0.001)
TCEP		−0.003	−0.169	−0.392
DTT		−0.003	−0.167	−0.391
TCEP + NEM	0.097	0.070	−0.129	−0.356
TCEP + BMPA	0.059	0.036	−0.153	−0.360

[a] All data are specific experimental points, rather than calculated from the modeling. As discussed in the text, rows 1−6 and rows 7 and 8 display equivalent values. Numbers in parentheses show the difference with the native protein.

of potentials as low as −0.85 V for up to 1 h, leading us to pursue the use of chemical reductants. Trialkylphosphines have been used widely to effect the two-electron reduction of disulfides on the surfaces of soluble proteins (*36*), and it was found that the disulfide bond in the *T. thermophilus* Rieske protein (Figure 1) was reduced to two free sulfhydryls by treatment with 10 mM TCEP [tris(2-carboxyethyl)-phosphine hydrochloride] at 60 °C for 1 h under anaerobic conditions (no other cysteines are present in the sequence). This procedure relies strongly on the thermostability of the protein, since shorter reaction times, or lower temperatures, did not result in complete conversion. Typical voltammetric signals recorded following disulfide reduction are shown in Figure 2B for comparison with those of the native protein in Figure 2A. Although the signals are decreased in intensity, the peaks remain compact and peak-to-peak separations remain small, though some extra broadening and separation occurs at the highest pHs. These effects may result from a change in the adsorption isotherm, a decrease in cluster content, and perhaps a decrease in the homogeneity of the cluster environment. Mutation of the two cysteine residues in other species has indicated that the disulfide bond is critical for either assembly or stability of the Rieske center (*18*−*20*), and a decrease in stability upon disulfide reduction may therefore be expected. Rinsing the film with water to ensure removal of any excess TCEP from the electrode surface did not affect the observed results, and reduction potentials recorded for the free sulfhydryl form changed by less than 10 mV over the 24 h following reduction, provided that the protein sample was kept anaerobic and at 4 °C. Control samples heated for 1 h at 60 °C, but in the absence of TCEP, produced voltammetric signals indistinguishable in either potential or intensity from those of the native protein (Table 1, row 2). A further control, in which the Rieske cluster was reduced using ascorbate, a single electron reductant with a higher potential, which does not affect the disulfide bond, also produced no changes in potential (Table 1, row 3).

Figure 3 compares the pH-dependent reduction potential of the Rieske center with the disulfide intact and with the disulfide reduced to two free sulfhydryl groups. Both curves in Figure 3 display the same fundamental shape and are fitted uniquely by the *E* and p*K* values defined by Scheme 1 and eqn 1; their numerical values are compared in Table 2. Disulfide reduction thus causes a decrease in $E^{0\prime}_{alk}$ and $E^{0\prime}_{acid}$ of 120 and 160 mV, respectively, and a corresponding increase in the p*K* values assigned to deprotonation of the two histidine ligands of 0.85 and 0.5 units for $pK_{ox1,2}$ and $pK_{red1,2}$, respectively. All voltammetric experiments on the TCEP-reduced form were recorded starting from a reducing potential poise to minimize any reoxidation of the free sulfhydryls before the experiment (see below). At low pH (<6) a more complex behavior than that displayed in Figure 2 was exhibited; while this is described separately below, the open squares in Figure 3 represent our best estimation of the reduction potential of the cluster with the two thiolates protonated: +0.14 V. Reduction of the disulfide bond with an alternative reagent, dithiothreitol (DTT), resulted in very similar changes in potential (Table 1, row 8), although the presence of DTT in solution produced significantly larger background currents than for TCEP. This necessitated extensive rinsing of the protein film after application to the surface; hence for convenience all further experiments were carried out using TCEP.

Table 2: Thermodynamic Parameters for the Various States of the Rieske Protein

	pK_{ox1}	pK_{ox2}	pK_{red1}	pK_{red2}	$E^{0\prime}_{acid}$	$E^{0\prime}_{alk}$
unmodified	7.85	9.65	12.5	12.5	0.161	−0.275
TCEP	8.7	10.5	13.0	13.0	0.000	−0.395
TCEP + NEM	8.5	9.9	12.9	12.9	0.075	−0.355
TCEP + BMPA	8.5	10.3	12.9	12.9	0.044	−0.363

Figure 4 compares the UV−visible spectra of three forms of the Rieske protein: oxidized, reduced with ascorbate, and reduced with TCEP. While voltammetric results (Table 1) clearly distinguish the state of the disulfide in these reduced forms, the optical spectra simply show that treatment with either ascorbate or TCEP reduces the iron−sulfur center; there is no apparent difference in the absorption spectra of the reduced proteins, merely a slight decrease in the cluster content of the TCEP-reduced protein which varies from sample to sample. Figure 5 presents the corresponding comparison of the EPR spectra of the reduced species. Samples reduced by ascorbate or dithionite produced virtually identical spectra, with $g_{x,y,z}$ values of 2.026, 1.901, and 1.802, in general agreement with values published previously for the *T. thermophilus* Rieske center (*4*, *37*, *38*), and other Rieske proteins (*1*). An additional narrow signal, at around $g = 2$, is present only in ascorbate-reduced samples. This

[3] Our inability to electrochemically *reduce* the native disulfide bond, even by poising at −0.85 V for 1 h, and the requirement for two-electron, chemical reductants are consistent with strongly irreversible voltammetry; electrochemical studies of thiols typically report irreversible behavior (*34*, *35*).

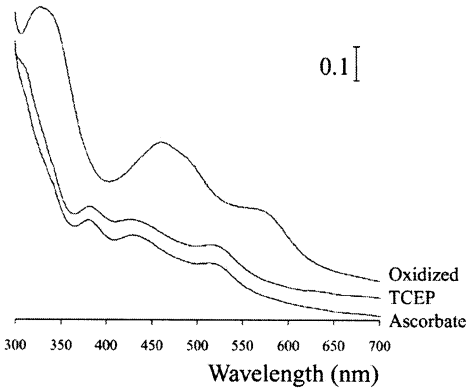

FIGURE 4: Comparison of the UV−visible spectra of the oxidized *T. thermophilus* Rieske protein, the protein reduced with 5 mM TCEP anaerobically for 1 h at 60 °C (both the cluster and the disulfide bond are reduced), and the protein reduced with 240 μM ascorbate (which reduces the cluster but leaves the disulfide bond intact). In all cases the same conditions were used: protein concentration approximately 80 μM, pH 7.5, buffer solution containing 0.1 M NaCl. The oxidized and TCEP-reduced proteins have been shifted upward by 0.05 and 0.1 absorbance units, respectively, for clarity.

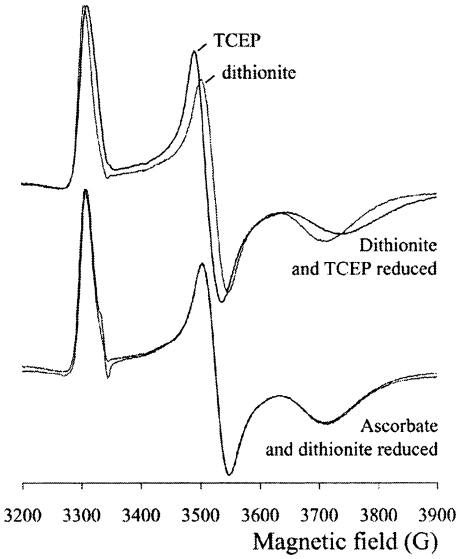

FIGURE 5: Comparison of EPR spectra of the *T. thermophilus* Rieske protein reduced with ascorbate or dithionite (which maintains the integrity of the disulfide bond) and with TCEP, which reduces the disulfide. Rieske protein (~100 μM, pH 7.5, 0.1 M NaCl) was reduced anaerobically by the addition of 0.4 mM ascorbate or dithionite or by incubation anaerobically at 60 °C for 1 h in the presence of 10 mM TCEP, and then immediately frozen. EPR conditions: microwave frequency 9.38 GHz, microwave power 0.2 mW, modulation amplitude 10 G, modulation frequency 100 kHz, time constant 10.24 ms, conversion time 40.96 ms, and sample temperature 33 K.

signal saturates rapidly as the microwave power is increased and is probably due to formation of a small amount of ascorbate free radical (*39*). Figure 5 also compares samples reduced by dithionite and TCEP. Overall, the two spectra are very similar; thus disulfide reduction has no more than a modulatory influence on the cluster electronic structure. However, two clear differences are consistently observed: (i) the peak corresponding to the g_z transition is broadened upon TCEP reduction, perhaps reflecting increased hyperfine interaction with the two Fe-liganded ^{14}N-nuclei, and (ii) small shifts are observed in the values of $g_{x,y,z}$ to 2.023, 1.907, and

Scheme 2: Summary of All Reactions of the Disulfide Bond and Thiols[a]

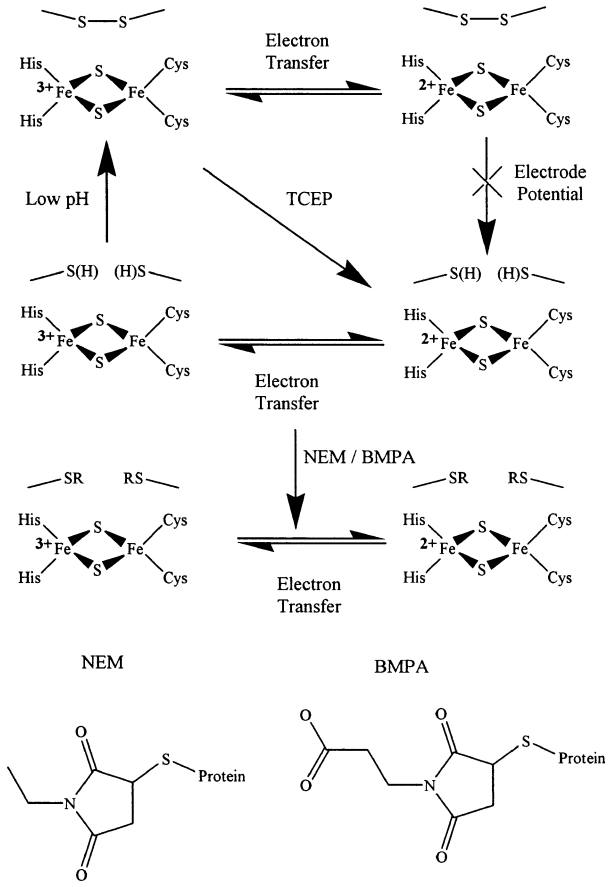

[a] Different protonation states of the Rieske cluster are not considered for simplicity, and parentheses are used to show that the free thiols may be either protonated or deprotonated, depending on the pH.

1.788, though g_{av} (=1.906) and these new values remain comfortably within the range of a typical Rieske-type center (*40*). Power saturation curves for all three species were essentially identical, with the signal being 50% saturated at ~100 mW and with no broadening below ~1 mW. Notably, the sole example of a disulfide cysteine mutant retaining an observable amount of cluster (<5%), the C155S mutation in the *R. capsulatus* cytochrome bc_1 complex (*19*), contains a cluster with altered physical characteristics similar to those reported here. The reduction potential is decreased by approximately 180 mV (pH not reported), and changes in the EPR spectrum are very similar: a slight shift in g_y from 1.89 to 1.90 and a much shallower g_z signal, shifted from 1.80 to approximately 1.77.

Alkylation of the Free Sulfhydryl Groups. The two free sulfhydryl groups formed by reaction with TCEP could be alkylated by incubation with standard reagents, as shown in Scheme 2 (*41*). Several reagents were tried: *N*-ethylmaleimide (NEM), *N*-β-maleimidopropionic acid (BMPA), *N*-benzylmaleimide (NBM), and iodoacetamide (IAA). The limited solubility of NBM in aqueous solution meant that nonaqueous solvents such as methanol were required to attain a high enough concentration; this requirement markedly decreased the stability of the protein films, and only limited information could be acquired in this case. For NEM, BMPA, and IAA stable and well-defined redox peaks were observed at all pHs, and examples recorded using NEM are shown in

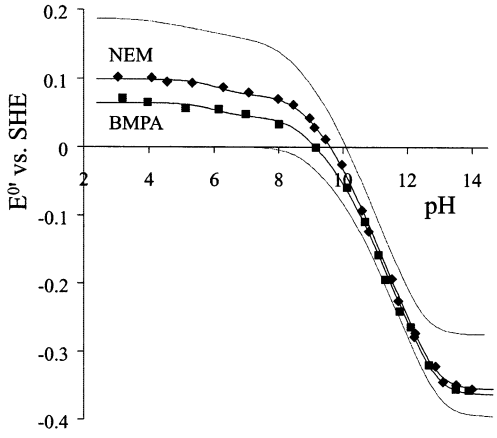

FIGURE 6: Variation of reduction potential with pH following alkylation of the free sulfhydryls by NEM (◆) or BMPA (■) compared to the potentials of the native and TCEP-reduced proteins from Figure 3. Fits to the data are using eq 1 and Scheme 1, and *E* and p*K* values are given in Table 2. Experimental conditions are as for Figure 2.

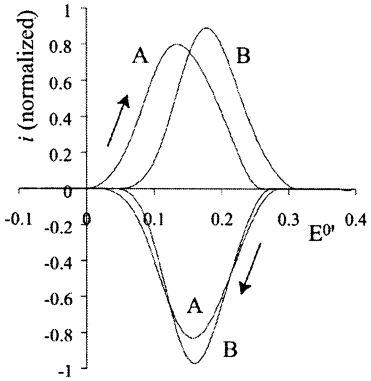

FIGURE 7: Voltammetric peaks from the first and tenth scan at low pH showing the positive shift in potential which occurs for the oxidative peak (from +0.133 to +0.186 V), the reductive peak remaining invariant in potential (+0.157 and +0.163 V). Conditions: pH 4.06, 2 M NaCl, and scan rate 0.1 V s^{-1}. All other conditions are as for Figure 2.

Figure 2C. Incubation of the native Rieske protein with NEM or BMPA alone (without TCEP pretreatment) produced only very small variations in reduction potential (Table 1, rows 4 and 5), but treatment with only IAA changed the observed reduction potentials significantly (~40 mV). Thus, in addition to reacting with free sulfhydryl groups, IAA reacts with other residues in the protein, such as His, Lys, Met, or Tyr, to a more significant extent than either NEM or BMPA. Therefore, only results from the maleimide reagents NEM and BMPA are considered.

The integrity of the reaction with NEM was confirmed by measurement of the intact mass of the Rieske protein in each state of modification: unmodified, treated with only NEM, and treated with both TCEP and NEM. Following reaction with only NEM the mass corresponding to the unmodified protein was observed,[4] along with several additional species with masses augmented by one, two, or three NEM residues (an extra mass of 125 Da each). Following treatment with TCEP first and then NEM, neither the unmodified protein mass or any mass augmented by one NEM could be observed, though masses corresponding to the addition of two, three, and four NEM groups were observed. The data are therefore in accord with the reaction scheme presented in Scheme 2. The overderivatized products are likely to result from nonspecific reactions and, since they are associated with only small variations in the reduction potential, are not considered further.

Upon alkylation of the free thiol groups, reversible signals could again be measured over the whole pH range, and the sample could be repeatedly cycled with no change in observed potential. The variation in reduction potential with pH is shown in Figure 6, following alkylation with either NEM or BMPA. The intrinsic p*K* and *E* values for the system, as defined in Scheme 1 and eq 1, are presented in Table 2. The potentials of both alkylated forms lie between the potentials of the native protein and the free sulfhydryl form; thus alkylation partially restores the high potential of the native protein. While both alkyl groups result in similar potentials, those of the NEM-derivatized protein are slightly higher than their BMPA-derivatized counterparts, particularly at lower pH.

Free Sulfhydryl Protonation and Recombination. (i) The Dithiol Form Can Be Reoxidized Voltammetrically to the Disulfide Form. At high pH, stable and reversible oxidation and reduction peaks (with small peak separations) are observed for the sulfhydryl form, but at low pH (<6) the behavior is complicated, and peak positions vary from one cycle to the next. Repeated cycling, however, generates a stable product, which displays reversible voltammetry and which retains invariant peak potentials over subsequent cycles. This same species can be generated by poising the sulfhydryl-protein film at positive potential (+0.4 V, 5 s) in a low-pH solution. Subsequent transfer of the protein-coated electrode into a solution of different pH (an "instant dialysis") thus allows measurement of the reduction potential over the whole pH range; results are presented in row 6 of Table 1. Since the product of the oxidative poise displays characteristics identical to those of the native protein, over the whole pH range, it is concluded to be the result of re-forming the disulfide bond. As recombination returns the protein to its native state, any environmental change in the vicinity of the cluster upon breaking (reduction) of the disulfide is reversible. Thus, observed changes in potential are unlikely to be due to large deformation or denaturation of the protein structure.

(ii) The Low-pH Sulfhydryl Form Is a Species Distinct from both the Native Protein and Its High-pH Counterpart. Figure 7 shows an example of the voltammetric peaks observed at low pH. Starting from a reducing potential, where the free sulfhydryls are stable, the potential is scanned in a positive direction, and a single oxidative peak is observed at ~+0.14 V. Unexpectedly, the reverse scan reveals the reductive peak potential to be more *positive* than its oxidative partner (~+0.16 V), showing clearly that a change to the cluster or its environment, which affects the reduction potential, has occurred at oxidizing potential (scan A). After several subsequent cycles, as discussed above, the two peaks reach the potentials exhibited by the native protein (scan B). The initial oxidative peak potential represents an *upper limit* for

[4] The mass of the unmodified protein was found to be 18386.0 (SD 1.0). This is 39 Da larger than the mass predicted from the sequence (18347.0), a difference which at present remains unaccounted for. Additional masses corresponding to deletion of the C-terminal residues TWRV and YTWRV were also observed in some preparations.

Scheme 3: Dependence of Thiol Recombination on the Redox and Protonation States of the Cluster and Thiols

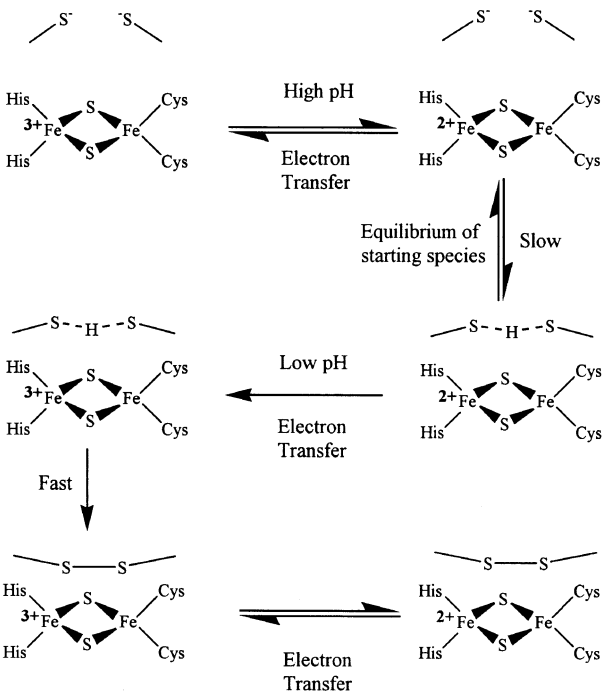

the reduction potential of the initial species since (i) the corresponding reductive peak would be more negative than its oxidative partner, under reversible conditions, and (ii) following reactions, coupled to cluster oxidation, would act to decrease the reduction potential. Oxidative peak potentials for the sulfhydryl form at 0.1 V s^{-1} are included in Figure 3 and are clearly separated from the higher average peak potentials of the native protein.

(iii) Conversion between the High- and Low-pH Sulfhydryl States. The high- and low-pH forms are clearly distinguishable in both potential and recombination kinetics, the disulfide being re-formed rapidly at low pH but much more slowly, or not at all, at high pH. Since this variation with pH is uniquely present when the two cysteines are present as free sulfhydryls (not with the cysteines disulfide bonded or alkylated), the apparent p*K* value of approximately 6.5, which describes the transition between high- and low-pH forms, most likely describes the addition of either one or two protons to the dithiolate pair. Voltammetric peaks at the pH transition are broad and difficult to distinguish from background, suggesting a slow equilibration between the protonated and deprotonated forms, with signal broadening resulting from the presence of two separate peaks; indeed, our best protein films have indicated this to be the case. However, since rates of protonation and deprotonation of the nearby cluster histidines, in the native protein, have so far proved too fast to measure by voltammetry, even at 500 V s^{-1} at pH 11 where an electron transfer requires the transfer of two protons, it is unlikely that proton expulsion or access to the disulfide vicinity is itself rate limiting (*35*). Scheme 3 presents our model for the pH dependency of the recombination rate: at low pH the two sulfhydryl groups are "preorganized" by the addition of one or two protons to the sulfhydryl pair (the slow conversion step), thus facilitating rapid disulfide formation upon cluster oxidation (*34*, *42*, *43*).

(iv) Dithiol to Disulfide Oxidation Occurs Only at Positive Electrode Potential. The lack of voltammetric reversibility exhibited by the TCEP-reduced protein at low pH (the apparent reduction potential is scan rate and scan number dependent) means that the *true* reduction potential cannot be defined by this experiment. In addition, increased scan rates aimed at "outrunning" the kinetics of recombination proved unsuccessful due to peak broadening rendering the peaks indistinguishable from background (*31*); this behavior of the TCEP-reduced form is in direct contrast to that of the native protein, for which reversible voltammetry was observed at scan rates up to 2000 V s^{-1}, and may result from disruption of the disulfide affecting the coupling between cluster and electrode. However, since the voltammetric response is independent of the length of time for which the potential is poised at reducing potential before the scan but very dependent on the duration and magnitude of any oxidative potential that is applied, it is clear that recombination either depends on cluster oxidation or results from direct sulfhydryl oxidation. The latter appears unlikely since the disulfide bond cannot be *reduced* directly by the electrode. The potential dependence of disulfide re-formation was estimated by applying a pulse of varying oxidative potential and then initiating a voltammetric scan from low potential to measure the degree of recombination (*44*). Results indicate that little or no disulfide formation occurs at any potential below 0 V, that thiol oxidation begins when potentials above +0.05 V are accessed, and that complete oxidation occurs very rapidly above +0.2 V. Qualitatively, these potentials correlate with the potential estimated for the cluster with the thiols protonated ($\leq$+0.14 V), again suggesting that thiol oxidation is dependent on cluster oxidation. Scheme 2 summarizes our model for the interconversion of oxidized and reduced forms of cluster and disulfide.

(v) Cluster and Thiols Are Both Oxidized Rapidly at Nominally the Same Potential. It has not proved possible to observe an additional oxidative peak, or an amplification of the cluster oxidative peak current, which could correspond to electron transfer from the two sulfhydryls to the electrode. There are two possible explanations: (i) the thiol oxidation peak is very broad and cannot be resolved from background, and (ii) while communication between cluster and thiols means that thiol oxidation depends on the cluster oxidation state, electrons are actually donated from the thiols to a solution species upon disulfide formation. Two pieces of evidence support the second hypothesis rather than the first: (a) the disulfide cannot be reduced directly by the electrode, making it unlikely that thiol oxidation occurs electrochemically; (b) the rate of recombination is fast, so slowing the voltammetric scan rate should have revealed a thiol−electrode electrode exchange (either direct or mediated by the cluster) if it were occurring. The identity of the proposed oxidant is currently unknown. Finally, more detailed investigations of the recombination kinetics and mechanism are currently precluded by our inability to maintain a consistent rate of thiol recombination between different preparations of the TCEP-reduced form (though reduction potentials remain completely reproducible) and by voltammetric peak broadening at high scan rate. The recombination reaction itself appears mechanistically complex, as may be expected for a system in which different protonation and electronation states of cluster and thiols interconvert in a pH-, time-, and potential-dependent fashion.

DISCUSSION

Dependence of Rieske Cluster Potential and H^+ Affinity upon Disulfide Bond Status. The [2Fe-2S] Rieske cluster, in all known structures, is sandwiched between two cysteine−histidine motifs on the $\beta6-\beta7/\beta4-\beta5$ loops that contribute two Cys (S^-) ligands to Fe1 and two His (N) ligands to Fe2 (*2*, *13*, *14*, *16*, *17*). In the high-potential, respiratory proteins, a disulfide bond also bridges these two loops in what may be considered a tether, and looking at Figure 1, one can imagine that this disulfide could "push" or "pull" the loops, thereby conferring special properties on the cluster. Current theories describing the function of the Rieske cluster in the respiratory cytochrome bc_1 and b_6f complexes involve electron transfer, and also perhaps proton transfer, from bound quinol. How the redox potential of the cluster and the p*K*s of the coordinated histidine imidazole rings are determined is therefore of central importance (*45*, *46*). Our results show that the thermodynamic stabilities of the oxidized cluster and the protonated histidines are increased upon reduction of the disulfide bond but that the spectral properties of the cluster are largely unchanged. Thus, with the two Cys side chains disulfide bonded, reduced to two free thiolates, or bisalkylated, it has been possible to explore the pH dependence of the cluster reduction potential over the range ~3−14. Below pH 6, with the reduced Cys in the protonated thiol form, disulfide bond formation occurs concurrently with cluster oxidation to regenerate the native protein.

A number of factors may contribute to changing the cluster environment upon reduction of the disulfide. These include relaxation of strain in the $\beta6-\beta7/\beta4-\beta5$ loop region and "across" the cluster, the introduction of two additional (thiolate) negative charges close to the cluster, and possible introduction of new strain, particularly in the bisalkylated form. The open squares in Figure 3 show our best estimation of the potential for the dithiol form, which is ≥0.04 V less than that of the native protein. Since the two SH groups do not differ greatly in charge or polarizability from the SS moiety, this decrease in potential, corresponding to ~4 kJ mol^{-1}, is considered to result from relaxation of strain effects in the cluster region. Referring to Figure 6, the nonionizable, bis-NEM form behaves very similarly to the native protein over the entire pH range (since alkylation removes the possibility of ionization), with $E^{0\prime}$ decreased by ~0.085 V; the additional small effects of bisalkylation are considered to be due to the bulky organic groups imposing new strain on the structure, causing a further relative stabilization of the oxidized cluster. The additional stabilization of the oxidized states, relative to the dithiol form, are ~4.3 kJ mol^{-1} upon NEM alkylation and 7.4−4.6 kJ mol^{-1} upon BMPA alkylation (depending on pH). As widely discussed in the literature, all of these may affect the reduction potential of the cluster by altering cluster solvation, hydrogen-bonding patterns, the proximity and orientation of amide and side chain dipoles, and the electrostatic interactions from charged residues (as modulated by the intervening dielectric) (*8*, *9*, *47*−*52*). Our evaluation of the observed changes, in terms of such considerations, follows.

First, cleavage of the disulfide bond might allow for increased solvent access to the cluster, particularly in the dithiolate form where the anions will repel one another. For iron−sulfur clusters, increases in solvent accessibility have been correlated with decreases in reduction potential and are commonly invoked to explain variations in potential within the same class of protein (*47*, *49*, *50*). Furthermore, it has been suggested that reduction potentials are dominated by a strong negative enthalpy change, characteristic of the class of protein, but modulated by an opposing negative entropy change (*53*). A major contributor to the entropy of reduction is the change in solvation with oxidation state; thus, if a reduction potential changes as a result of increased solvent accessibility, a corresponding increase in the entropy of reduction is expected (*47*, *53*, *54*). Entropies of reduction for the native and free sulfhydryl proteins were therefore measured from the temperature dependence of their reduction potentials at pH 7, 7.5, and 8 (chosen to be in the pH-independent region to avoid protonation effects dominating). The two values, −48 (±5) J K^{-1} mol^{-1}, were indistinguishable within experimental error (data not shown) (*7*), demonstrating that the change in reduction potential is enthalpic, rather than entropic, in origin. Thus the observed decrease in reduction potential is unlikely to be due to increased solvation of the cluster. Our results are quite different from those of Osyczka and co-workers, who found that the potential of the *R. capsulatus* cytochrome c_1, decreased by over 300 mV upon removal of an adjacent disulfide bond, could be raised almost back to its native value by the addition of a β-branched amino acid two residues away, effects attributed to changes in solvent access to the active site (*55*).

Second, changes in hydrogen-bonding and amide dipole interactions may result from releasing the disulfide tether. Since there is no direct structural information available on the effects of reducing the disulfide, our model is the structure of the low-potential Rieske protein from *Burkholderia* sp. strain LB400 biphenyl dioxygenase [PDB Accession No. 1FQT (*5*, *16*)], which has a highly similar, overall cluster fold (and solvent accessibility) but in which the cysteines of the disulfide bond are replaced by a tryptophan and a leucine, in van der Waals contact. Three hydrogen-bonding interactions, present in the high-potential Rieske protein, are absent from the low-potential protein; two result from rearrangement of the three residues immediately preceding the first disulfide cysteine and the third from a change in orientation associated with replacing the second cysteine (*16*). While quantitative predictions of the effect of a hydrogen bond on reduction potential are difficult, the combined effect of three bonds could easily account for the estimated decrease of ≥0.04 V (*8*, *9*, *48*−*50*). Indeed, the effect of removing the hydrogen bond from the conserved Ser or Tyr residues in the Rieske proteins from *Paracoccus denitrificans* and *S. cerevisae* ranges between 0.045 and 0.13 V (*8*, *9*). Note, however, that subtle differences in the structures of the two proteins may also contribute to determining their hydrogen-bonding patterns.

Finally, at higher pH, the negative charges on the deprotonated thiols interact electrostatically with the cluster and the histidine ligands, promoting a decrease in the cluster reduction potential and an increase in the histidine p*K* values. The behavior shown in Figure 3 fits well with this simple prediction and indicates that thiol deprotonation occurs above pH 6.5 (±1). As reported in Table 2, the cluster potential decreases by a total of 0.16−0.12 V (depending on whether the histidines are protonated), and the histidine p*K*s increase by 0.85 to 0.5 (depending on cluster oxidation state). The

extra effect on the reduction potential of 0.12−0.08 V corresponds to 11.6−7.7 kJ mol^{-1}, whereas the analogous free energy changes associated with changing the p*K* values are 4.8−2.8 kJ mol^{-1}; this reflects the spatial separation and distinct environments of the redox and protonation sites. Our estimate of 6.5 for the p*K* of either one or both free thiols is lower than the p*K* of a typical cysteine thiol (8.7) and at the lower end of the range typically exhibited by other alkanethiols (7−11) (*29*, *56*). However, cysteine p*K*s are, like cluster redox potential, subject to variation in electrostatic, dipolar, and hydrogen-bonding interactions and solvent accessibility, and there are numerous examples of protein thiols with p*K* values below 6; the reactive thiols in DsbA and glutaredoxin have p*K* values as low as 3.5 (*43*, *57*, *58*).

Interactions between Free Thiols and Cluster Oxidation State: Re-Formation of the Disulfide Bond. The rate of oxidative recombination of the two free thiols is strongly pH dependent, occurring rapidly at low pH but more slowly, if at all, as the pH is increased. This is opposite to the behavior usually associated with disulfide formation, since thiol *exchange* reactions are faster at higher pH due to the requirement for a deprotonated thiol nucleophile (*43*, *56*). Formation of the Rieske protein disulfide, however, is not an exchange reaction, but a direct oxidation reaction, and is thus not confined to a mechanism involving nucleophilic attack. Instead, as shown in Scheme 3, the increased recombination rate upon thiol protonation may reflect preorganization of the two free thiols, which, when protonated, no longer electrostatically repel one another and may even interact by hydrogen bonding (*34*, *43*). Thiol protonation at pH ∼6.5 may involve addition of either one or two protons to the thiol pair; proton sharing has been reported for the thiol pair in *E. coli* thioredoxin and for several other pairs of acidic residues (*42*).

In addition to the pH dependence of the recombination rate, there is also a clear dependence on electrode potential. This is indicated by the fact that the thiols are stable when the cluster is reduced but rapidly convert to the disulfide upon application of an oxidative potential (>0.00 V). Furthermore, voltammetric experiments at low pH have been unable to separate thiol oxidation from cluster oxidation; faster scan rates did not succeed in outrunning thiol oxidation (to measure the reversible potential of the cluster) nor did placing a limit on the potential range isolate the oxidation of only one of the two redox couples. Instead, cluster and thiols are both oxidized rapidly, at nominally the same potential.

Typical redox potentials for the disulfide−thiol couple lie in the range −0.4 to −0.2 V (pH 7), with the highest values around −0.12 V reported for *E. coli* DsbA and protein disulfide isomerase (PDI) (*34*, *43*); a value for the Rieske protein thiols has not been determined, but since disulfide formation is likely to be sterically favored and there is little dihedral strain in the disulfide bond [∼90° (*34*, *43*)], the potential is likely to tend toward the lower end of the range. Thiol oxidation at +0.14 V is therefore at significant overpotential. It is highly unlikely that thiol oxidation occurs directly at the electrode, since no corresponding oxidative signal is observed and since disulfide bond reduction cannot be brought about electrochemically. Moreover, since there is no amplification of the cluster oxidation current, despite recombination being very rapid, there is no concrete evidence to support the hypothesis that the cluster is able to mediate electron transfer between the thiols and the electrode. The remaining possibility is the participation of an unidentified solution species oxidant. However, thiol oxidation *is dependent* upon cluster oxidation, so that the two occur concurrently; thus the cluster has a defining influence upon the recombination of the disulfide, even if not directly involved in channeling electrons out to the electrode.

Why a Disulfide? Finally, our results have possible relevance to the broader questions concerning biosynthesis of the protein and its function within the respiratory complexes. First, the point of disulfide incorporation is currently unknown, and while disulfide formation is promoted in the oxidizing environment of the bacterial periplasm (*59*, *60*), this is not true of the mitochondrial intermembrane space in redox contact with the cytosol. Additionally, it is not known whether soluble, overexpressed Rieske proteins, retained in the reducing cytoplasm of *E. coli* (−0.27 V), display native disulfide incorporation or whether the disulfide forms during aerobic purification (*7*, *14*). However, it is known that in bacteria the bc_1−Rieske protein is exported from the cytoplasm fully folded, with an intact iron−sulfur cluster, via the TAT pathway (*61*), whereas low-potential Rieske proteins, which do not require the disulfide, are retained in the cytoplasm.

Second, the ability of 2,3-dimercaptopropanol (BAL) to either destroy the Rieske iron−sulfur cluster or prevent its reduction in a normal fashion (*62*) suggests the need to maintain the disulfide intact during catalysis. The modification of the Rieske cluster EPR spectrum upon disulfide reduction is similar to that observed in the intact bc_1 complex in response to changes in the redox potential of the Q pool and Q_O site occupancy, changes in the position of the Rieske subdomain at the Q_O site, and upon binding of stigmatellin (*63*−*65*). It is also becoming clear that binding of QH_2 in the Q_O site involves a hydrogen bond to one of the Rieske cluster histidine ligands; this may facilitate electron transfer, and perhaps proton transfer, from the bound quinol to the cluster (*45*, *46*, *64*). Finally, the <5% cluster present in the *R. capsulatus* C155S mutant displayed a decreased potential and could not bind stigmatellin or sense the redox state of the Q pool (*19*). Taken together, these observations strongly suggest a role for the disulfide bond in maintaining the conformation of the Q_O site and the integrity of the hydrogen-bonding network therein and, thus, in quinol binding.

Third, the possible role of the conserved disulfide in the electron/proton transfer functions within the respiratory complex has been little discussed. Most obviously, the disulfide might aid in raising the redox potential and decreasing the histidines' p*K*s; both are required to be optimized for maximal cytochrome bc_1/b_6f complex activity (*45*, *46*, *63*). However, our work has shown that the influence of the disulfide, particularly when converted to two *neutral* ligands, is only small, and thus if a functional cytochrome bc_1 complex lacking the disulfide could be produced, any effect on catalysis would be unlikely to be due to alteration of the redox potential. Our results have also demonstrated that the redox and protonation states of the cluster affect, and are affected by, the redox and protonation states of the disulfide; in particular, thiol oxidation, to re-form the disulfide, is controlled by cluster oxidation. This tentatively suggests a role for the disulfide as an electron/proton transfer

agent, perhaps in protecting the cluster from attack by reactive oxygen species generated at the Q_O site. Finally, this communication between the Rieske cluster and the disulfide provides a direct link between the redox potential of the electron transport chain and the potentials of the cellular thiol/disulfide pools, implying a possible regulatory function.

ACKNOWLEDGMENT

We thank Dr. Ian M. Fearnley for carrying out mass spectrometry measurements and Professors Fraser A. Armstrong and P. Leslie Dutton for helpful discussions.

REFERENCES

1. Link, T. A. (1999) The structures of Rieske and Rieske-type proteins, *Adv. Inorg. Chem. 47*, 83−157.
2. Iwata, S., Saynovits, M., Link, T. A., and Michel, H. (1996) Structure of a water soluble fragment of the 'Rieske' iron−sulfur protein of the bovine heart mitochondrial cytochrome bc_1 complex determined by MAD phasing at 1.5 Å resolution, *Structure 4*, 567−579.
3. Gurbiel, R. J., Batie, C. J., Sivaraja, M., True, A. E., Fee, J. A., Hoffman, B. M., and Ballou, D. P. (1989) Electron−nuclear double resonance spectroscopy of ^{15}N-enriched phthalate dioxygenase from *Pseudomonas cepacia* proves that two histidines are coordinated to the [2Fe-2S] Rieske-type clusters, *Biochemistry 28*, 4861−4871.
4. Fee, J. A., Findling, K. L., Yoshida, T., Hille, R., Tarr, G. E., Hearshen, D. O., Dunham, W. R., Day, E. P., Kent, T. A., and Münck, E. (1984) Purification and characterization of the Rieske iron−sulfur protein from *Thermus thermophilus*, *J. Biol. Chem. 259*, 124−133.
5. Couture, M. M.-J., Colbert, C. L., Babini, E., Rosell, F. I., Mauk, A. G., Bolin, J. T., and Eltis, L. D. (2001) Characterization of BphF, a Rieske-type ferredoxin with a low reduction potential, *Biochemistry 40*, 84−92.
6. Zhang, H., Carrell, C. J., Huang, D., Sled, V., Ohnishi, T., Smith, J. L., and Cramer, W. A. (1996) Characterization and crystallization of the lumen side domain of the chloroplast Rieske iron−sulfur protein, *J. Biol. Chem. 271*, 31360−31366.
7. Zu, Y., Fee, J. A., and Hirst, J. (2001) Complete thermodynamic characterization of reduction and protonation of the bc_1-type Rieske [2Fe-2S] center of *Thermus thermophilus*, *J. Am. Chem. Soc. 123*, 9906−9907.
8. Schröter, T., Hatzfeld, O. M., Gemeinhardt, S., Korn, M., Friedrich, T., Ludwig, B., and Link, T. A. (1998) Mutational analysis of residues forming hydrogen bonds in the Rieske [2Fe-2S] cluster of the cytochrome bc_1 complex in *Paracoccus denitrificans*, *Eur. J. Biochem. 255*, 100−106.
9. Denke, E., Merbitz-Zahradnik, T., Hatzfeld, O. M., Snyder, C. H., Link, T. A., and Trumpower, B. L. (1998) Alteration of the midpoint potential and catalytic activity of the Rieske iron−sulfur protein by changes of amino acids forming hydrogen bonds to the iron−sulfur cluster, *J. Biol. Chem. 273*, 9085−9093.
10. Link, T. A. (1994) Two p*K* values of the oxidized 'Rieske' [2Fe-2S] cluster observed by CD spectroscopy, *Biochim. Biophys. Acta 1185*, 81−84.
11. Kuila, D., Schoonover, J. R., Dyer, R. B., Batie, C. J., Ballou, D. P., Fee, J. A., and Woodruff, W. H. (1992) Resonance Raman studies of Rieske-type proteins, *Biochim. Biophys. Acta 1140*, 175−183.
12. Link, T. A., Hatzfeld, O. M., Unalkat, P., Shergill, J. K., Cammack, R., and Mason, J. R. (1996) Comparison of the 'Rieske' [2Fe-2S] center in the bc_1 complex and in bacterial dioxygenases by circular dichroism spectroscopy and cyclic voltammetry, *Biochemistry 35*, 7546−7552.
13. Carrell, C. J., Zhang, H., Cramer, W. A., and Smith, J. L. (1997) Biological identity and diversity in photosynthesis and respiration: structure of the lumen-side domain of the chloroplast Rieske protein, *Structure 5*, 1613−1625.
14. Bönisch, H., Schmidt, C. L., Schäfer, G., and Ladenstein, R. (2002) The structure of the soluble domain of an archaeal Rieske iron−sulfur protein at 1.1 Å resolution, *J. Mol. Biol. 319*, 791−805.
15. Hunsicker-Wang, L., Heine, A., Chen, Y., Luna, E., Todaro, T., Zhang, Y., Williams, P. A., McRee, D., Stout, C. D., and Fee, J. A. (2002) manuscript in preparation.
16. Colbert, C. L., Couture, M. M.-J., Eltis, L. D., and Bolin, J. T. (2000) A cluster exposed: structure of the Rieske ferredoxin from biphenyl dioxygenase and the redox properties of Rieske FeS proteins, *Structure 8*, 1267−1278.
17. Kauppi, B., Lee, K., Carredano, E., Parales, R. E., Gibson, D. T., Eklund, H., and Ramaswamy, S. (1998) Structure of an aromatic-ring-hydroxylating dioxygenase−naphthalene 1,2-dioxygenase, *Structure 6*, 571−586.
18. Van Doren, S. R., Gennis, R. B., Barquera, B., and Crofts, A. R. (1993) Site-directed mutations of conserved residues of the Rieske iron−sulfur subunit of the cytochrome bc_1 complex of *Rhodobacter sphaeroides* blocking or impairing quinol oxidation, *Biochemistry 32*, 8083−8091.
19. Davidson, E., Ohnishi, T., Atta-Asafo-Adeji, E., and Daldal, F. (1992) Potential ligands to the [2Fe-2S] Rieske cluster of the cytochrome bc_1 complex of *Rhodobacter capsulatus* probed by site-directed mutagenesis, *Biochemistry 31*, 3342−3351.
20. Graham, L. A., and Trumpower, B. L. (1991) Mutational analysis of the mitochondrial Rieske iron−sulfur protein of *Saccharomyces cerevisae*, *J. Biol. Chem. 266*, 22485−22492.
21. Dai, S., Schwendtmayer, C., Schürmann, P., Ramaswamy, S., and Eklund, H. (2000) Redox signaling in chloroplasts: cleavage of disulfides by an iron−sulfur cluster, *Science 287*, 655−658.
22. Staples, C. R., Ameyibor, E., Fu, W., Gardet-Salvi, L., Stritt-Etter, A.-L., Schürmann, P., Knaff, D. B., and Johnson, M. K. (1996) The function and properties of the iron−sulfur center in spinach ferredoxin:thioredoxin reductase: a new biological role for iron−sulfur clusters, *Biochemistry 35*, 11425−11434.
23. Staples, C. R., Gaymard, E., Stritt-Etter, A.-L., Telser, J., Hoffman, B. M., Schürmann, P., Knaff, D. B., and Johnson, M. K. (1998) Role of the $[Fe_4S_4]$ cluster in mediating disulfide reduction in spinach ferredoxin:thioredoxin reductase, *Biochemistry 37*, 4612−4620.
24. Duin, E. C., Madadi-Kahkesh, S., Hedderich, R., Clay, M. D., and Johnson, M. K. (2002) Heterodisulfide reductase from *Methanothermobacter marburgensis* contains an active-site [4Fe-4S] cluster that is directly involved in mediating heterodisulfide reduction, *FEBS Lett. 512*, 263−268.
25. Armstrong, F. A. (1997) Evaluations of reduction potential data in relation to coupling, kinetics and function, *J. Biol. Inorg. Chem. 2*, 139−142.
26. Armstrong, F. A., Heering, H. A., and Hirst, J. (1997) Reactions of complex metalloproteins studied by protein-film voltammetry, *Chem. Soc. Rev. 26*, 169−179.
27. Gatti, D. L., Tarr, G., Fee, J. A., and Ackerman, S. H. (1998) Cloning and sequence analysis of the structural gene for the bc_1-type Rieske iron−sulfur protein from *Thermus thermophilus* HB8, *J. Bioenerg. Biomembr. 30*, 223−233.
28. Bard, A. J., and Faulkner, L. R. (2001) in *Electrochemical Methods*, 2nd ed., Wiley, New York.
29. Lide, D. R. (2000) in *Handbook of Chemistry and Physics*, 81st ed., CRC Press, Boca Raton, FL.
30. Taniguchi, V. T., Sailasuta-Scott, N., Anson, F. C., and Gray, H. B. (1980) Thermodynamics of metalloprotein electron-transfer reactions, *Pure Appl. Chem. 52*, 2275−2281.
31. Hirst, J., and Armstrong, F. A. (1998) Fast-scan cyclic voltammetry of protein films on pyrolytic graphite edge electrodes: characteristics of electron exchange, *Anal. Chem. 70*, 5062−5071.
32. Clark, W. M. (1960) in *Oxidation−reduction potentials of organic systems*, Williams and Wilkins, Baltimore, MD.
33. Zu, Y., Di Bernardo, S., Yagi, T., and Hirst, J. (2002) Redox properties of the [2Fe-2S] center in the 24 kDa (NQO2) subunit of NADH:ubiquinone oxidoreductase (complex I), *Biochemistry 41*, 10056−10069.
34. Gilbert, H. F. (1997) Thiol/disulfide exchange and redox potentials of proteins, in *Bioelectrochemistry of Biomacromolecules* (Lenaz, G., and Milazzo, G., Eds.) pp 256−324, Birkhäuser Verlag, Switzerland.
35. Shouji, E., and Buttry, D. A. (1999) A mechanistic study of the influence of proton-transfer processes on the behavior of thiol/disulphide redox couples, *J. Phys. Chem. B 103*, 2239−2247.
36. Kirley, T. L. (1989) Reduction and fluorescent labeling of cyst-(e)ine-containing proteins for subsequent structural analyses, *Anal. Biochem. 180*, 231−236.

37. Kuila, D., and Fee, J. A. (1986) Evidence for a redox linked ionizable group associated with the [2Fe-2S] cluster of *Thermus* Rieske protein, *J. Biol. Chem. 261*, 2768−2771.
38. Cline, J. F., Hoffman, B. M., Mims, W. B., LaHaie, E., Ballou, D. P., and Fee, J. A. (1985) Evidence for N coordination to Fe in the [2Fe-2S] clusters of *Thermus* Rieske protein and phthalate dioxygenase from *Pseudomonas*, *J. Biol. Chem. 260*, 3251−3254.
39. Van Duijn, M. M., Van der Zee, J., and Van den Broek, P. J. A. (1998) Electron spin resonance study on the formation of ascorbate free radical from ascorbate: the effect of dehydroascorbic acid and ferricyanide, *Protoplasma 205*, 122−128.
40. Bertrand, P., Guigliarelli, B., Gayda, J.-P., Beardwood, P., and Gibson, J. F. (1985) A ligand-field model to describe a new class of 2Fe-2S clusters in proteins and their synthetic analogues, *Biochim. Biophys. Acta 831*, 261−266.
41. Dawson, R. M. C., Elliott, D. C., Elliott, W. H., and Jones, K. M. (1990) in *Data for Biochemical Research*, 3rd ed., Oxford University Press, Oxford.
42. Jeng, M.-F., Holmgren, A., and Dyson, H. J. (1995) Proton sharing between cysteine thiols in *Escherichia coli* thioredoxin: implications for the mechanism of protein disulfide reduction, *Biochemistry 34*, 10101−10105.
43. Gilbert, H. F. (1990) Molecular and cellular aspects of thiol−disulfide exchange, *Adv. Enzymol. 63*, 69−172.
44. Camba, R., and Armstrong, F. A. (2000) Investigations of the oxidative disassembly of Fe−S clusters in *Clostridium pasteurianum* 8Fe ferredoxin using pulsed-protein-film voltammetry, *Biochemistry 39*, 10587−10598.
45. Crofts, A. R., Hong, S., Ugulava, N., Barquera, B., Gennis, R., Guergova-Kuras, M., and Berry, E. A. (1999) Pathways for proton release during ubihydroquinone oxidation by the bc_1 complex, *Proc. Natl. Acad. Sci. U.S.A. 96*, 10021−10026.
46. Hong, S., Ugulava, N., Guergova-Kuras, M., and Crofts, A. R. (1999) The energy landscape for ubihydroquinone oxidation at the Q_O site of the bc_1 complex in *Rhodobacter sphaeroides*, *J. Biol. Chem. 274*, 33931−33944.
47. Capozzi, F., Ciurli, S., and Luchinat, C. (1998) Coordination sphere versus protein environment as determinants of electronic and functional properties of iron−sulfur proteins, *Struct. Bonding 90*, 127−160.
48. Low, D. W., and Hill, M. G. (2000) Backbone-engineered high-potential iron proteins: effects of active-site hydrogen bonding on reduction potential, *J. Am. Chem. Soc. 122*, 11039−11040.
49. Backes, G., Mino, Y., Loehr, T. M., Meyer, T. E., Cusanovich, M. A., Sweeney, W. V., Adman, E. T., and Sanders-Loehr, J. (1991) The environment of Fe_4S_4 clusters in ferredoxins and high-potential iron proteins. New information from X-ray crystallography and resonance Raman spectroscopy, *J. Am. Chem. Soc. 113*, 2055−2064.
50. Jensen, G. M., Warshel, A., and Stephens, P. J. (1994) Calculation of the redox potentials of iron−sulfur proteins: the 2-/3-couple of [$Fe_4S_4Cys_4$] clusters in *Peptococcus aerogenes* ferredoxin, *Azotobacter vinelandii* ferredoxin I, and *Chromatium vinosum* high-potential iron protein, *Biochemistry 33*, 10911−10924.
51. Gunner, M. R., and Honig, B. (1991) Electrostatic control of midpoint potentials in the cytochrome subunit of the *Rhodopseudomonas viridis* reaction center, *Proc. Natl. Acad. Sci. U.S.A. 88*, 9151−9155.
52. Chen, K., Bonagura, C. A., Tilley, G. J., McEvoy, J. P., Jung, Y.-S., Armstrong, F. A., Stout, C. D., and Burgess, B. K. (2002) Crystal structures of ferredoxin variants exhibiting large changes in [Fe-S] reduction potential, *Nat. Struct. Biol. 9*, 188−192.
53. Battistuzzi, G., D'Onofrio, M., Borsari, M., Sola, M., Macedo, A. L., Moura, J. J. G., and Rodrigues, P. (2000) Redox thermodynamics of low-potential iron−sulfur proteins, *J. Biol. Inorg. Chem. 5*, 748−760.
54. Dunitz, J. D. (1994) The entropic cost of bound water in crystals and biomolecules, *Science 264*, 670−671.
55. Osyczka, A., Dutton, P. L., Moser, C. C., Darrouzet, E., and Daldal, F. (2001) Controlling the functionality of cytochrome c_1 redox potentials in the *Rhodobacter capsulatus* bc_1 complex through disulfide anchoring of a loop and a β-branched amino acid near the heme-ligating methionine, *Biochemistry 40*, 14547−14556.
56. Gough, J. D., Williams, R. H., Donofrio, A. E., and Lees, W. J. (2002) Folding disulfide-containing proteins faster with an aromatic thiol, *J. Am. Chem. Soc. 124*, 3885−3892.
57. Nelson, J. W., and Creighton, T. E. (1994) Reactivity and ionization of the active site cysteine residues of DsbA, a protein required for disulfide bond formation in vivo, *Biochemistry 33*, 5974−5983.
58. Darby, N. J., and Creighton, T. E. (1995) Characterization of the active site cysteine residues of the thioredoxin-like domains of protein disulfide isomerase, *Biochemistry 34*, 16770−16780.
59. Glockshuber, R. (1999) Where do the electrons go? *Nature 401*, 30−31.
60. Debarbieux, L., and Beckwith, J. (1999) Electron avenue: pathways of disulfide bond formation and isomerization, *Cell 99*, 117−119.
61. Berks, B. C., Sargent, F., and Palmer, T. (2000) The Tat protein export pathway, *Mol. Microbiol. 35*, 260−274.
62. Slater, E. C., and de Vries, S. (1980) Identification of the BAL-labile factor, *Nature 288*, 717−718.
63. Darrouzet, E., Valkova-Valchanova, M., and Daldal, F. (2002) The [2Fe-2S] cluster E_m as an indicator of the iron−sulfur subunit position in the ubihydroquinone oxidation site of the cytochrome bc_1 complex, *J. Biol. Chem. 277*, 3464−3470.
64. Samiolova, R. I., Kolling, D., Uzawa, T., Iwasaki, T., Crofts, A. R., and Dikanov, S. A. (2002) The interaction of the Rieske iron−sulfur protein with occupants of the Q_O-site of the bc_1 complex, probed by electron spin−echo envelope modulation, *J. Biol. Chem. 277*, 4605−4608.
65. Robertson, D. E., Daldal, F., and Dutton, P. L. (1990) Mutants of ubiquinol-cytochrome c_2 oxidoreductase resistant to Q_O site inhibitors: consequences for ubiquinone and ubiquinol affinity and catalysis, *Biochemistry 29*, 11249−11260.

BI026589R